ACS Sustainable Chemistry & Engineering

Research Article

Cite This: ACS Sustainable Chem. Eng. 2019, 7, 15928−15938

pubs.acs.org/journal/ascecg

Understanding Laccase−Ionic Liquid Interactions toward Biocatalytic Lignin Conversion in Aqueous Ionic Liquids

Joseph C. Stevens,[†] Lalitendu Das,[†,∥] Justin K. Mobley,[‡] Shardrack O. Asare,[‡] Bert C. Lynn,[‡] David W. Rodgers,[§] and Jian Shi*[,†]

[†]Department of Biosystems and Agricultural Engineering, University of Kentucky, 128 C.E. Barnhart Building, Lexington, Kentucky 40506, United States

[‡]Department of Chemistry, University of Kentucky, 125 Chemistry/Physics Building, Lexington, Kentucky 40506, United States

[§]Department of Molecular and Cellular Biochemistry, University of Kentucky, 277 BBSRB Building, Lexington, Kentucky 40536, United States

Supporting Information

ABSTRACT: Lignin is a crucial component of plant matter; however, it is also largely responsible for the recalcitrance of lignocellulosic biomass when subjected to pretreatment processes. Lignin is generated in large volumes as a waste product from paper and pulping industry as well as cellulosic biorefineries. As a result, lignin valorization is critical to the successful implementation of cellulosic biofuels. To this end, we investigated interactions between three ionic liquids (ILs) and the lignolytic enzyme laccase toward biocatalytic lignin conversion to aromatic monomers. Laccase exhibited minimal loss of activity in 10% diethylamine hydrogensulfate ([DEA][HSO_4]). Changes in V_{max} and K_m of laccase with respect to IL concentration indicate that [DEA][HSO_4] is a noncompetitive inhibitor, whereas cholinium lysinate ([Ch][Lys]) and [C_2C_1Im][OAc] are mixed inhibitors. Docking simulations suggested that [Ch][Lys] and [C_2C_1Im][OAc] disrupt residues leading to the active site. Experiments with a β-O-4′ linked model dimer revealed that laccase in [C_2C_1Im][OAc] and [Ch][Lys] requires the presence of 2,2′-azino-bis(3-ethylbenzothiazoline-6-sulfonic acid) (ABTS) to oxidize the β-O-4′ linkage, leading to polymerization of the model dimer. Alkaline lignin treated with laccase, ABTS, and the aqueous ILs (AILs) showed few structural changes, although the lignin was partially solubilized and converted to degradation products. The major products obtained from alkaline lignin were vanillin, acetosyringone, syringaldehyde, and acetovanillone. The results of this study provide, for the first time, an in-depth explanation of the interactions between laccase and AILs for the purpose of lignin valorization.

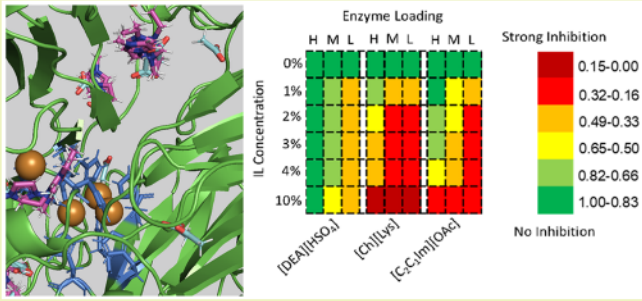

KEYWORDS: *biocatalysis, lignin, laccase, ionic liquid, docking*

INTRODUCTION

Lignin is among the most abundant biopolymers found in nature and makes up around one-quarter of lignocellulosic biomass.[1−3] Lignin is primarily made of three phenylpropanoid subunits synthesized from corresponding alcohol precursors: *p*-coumaryl alcohol (H), coniferyl alcohol (G), and sinapyl alcohol (S).[4,5] These monolignols are joined via a complex network of linkages including β-aryl ether (β-O-4′), phenylcoumaran (β-5′), and resinol ($\beta-\beta'$) as the dominant linkages.[6,7] The nature of the linkages is largely determined by the monolignol content of the biomass which, in turn, is dependent upon the source of the biomass.[8] The compositional and structural heterogeneity contributes largely to lignin's recalcitrance to biological or chemical decomposition. Currently, lignin is generated in large volume as a waste product from the paper and pulping industry as well as a byproduct of the cellulosic biorefineries.[9,10] Developing technologies to convert lignin to value-added products will not only reduce waste generation but also increase revenue for the paper industry as well as future cellulosic biorefineries.[11,12]

Lignin has limited use in its polymeric form. In contrast, the phenolic compounds derived from lignin depolymerization can be used as fuels or building blocks to synthesize chemicals for the food, plastic, and pharmaceutical industries, which are, at present, primarily derived from petroleum.[13−15] Lignin depolymerization methods can be categorized into thermochemical, such as high-temperature pyrolysis, hydrogenolysis, and catalytic oxidation, and biological, that is using lignolytic enzymes or microbes.[16−19] In general, biological lignin depolymerization can be performed at milder temperatures and pressures compared to thermochemical methods, potentially improving product selectivity via the specificity of the

Received: April 17, 2019
Revised: August 19, 2019
Published: September 3, 2019

DOI: 10.1021/acssuschemeng.9b02151
ACS Sustainable Chem. Eng. 2019, 7, 15928−15938

biocatalysts.[17,20] A range of lignin degrading enzymes (LDEs) have been investigated including lignin peroxidases, versatile peroxidases, manganese peroxidases, laccases from white and brown rot fungi, and the newly discovered NAD or glutathione-dependent enzymes from certain soil bacteria, such as *Sphingobium SYK-6*.[21−23] However, application of these lignolytic enzymes in large-scale operations valorizing lignin to aromatic monomers is still hindered due to the high cost of enzyme production and poor yield of aromatic monomers due to the very low lignin solubility (for many of the industrially derived technical lignin) in the aqueous environment compatible with enzyme activity as well as the poor selectivity of the lignolytic enzymes to produce defined monomers.[24,25]

Most of the known effective lignin solvents [e.g., dimethyl sulfoxide (DMSO), acetone, or alkaline solutions] are detrimental to enzyme activity when added to aqueous solutions.[26,27] In addition, they often require high temperature for complete lignin dissolution, especially when dealing with plant-derived native lignins,[28] which again can be incompatible with the use of enzymes. Thus, a solvent system with both high lignin solubility and enzyme compatibility is preferred for developing a better biological lignin depolymerization process. Ionic liquids (ILs) are molten salts made of organic cations and anions that are liquid at temperatures < 100 °C.[29] By selecting the cation and anion, the properties of an IL can be tuned for a wide range of applications.[30−32] Alkylimidazolium-based ILs have been extensively studied for biomass pretreatment and lignin fractionation.[33−35] Recently, ILs from bioderived cations (such as choline and ammonium) and anions (such as amino acids and carboxylic acids) have been investigated as lower-cost alternatives to imidazolium-based ILs.[36] For example, pretreating switchgrass with 10% cholinium lysinate ([Ch][Lys]) in water resulted in >80% of the lignin being solubilized into the liquid stream.[37] Results also suggest that tuning aqueous IL (AIL) mixtures can favor specific products during a catalytic oxidation process.[38]

Laccases are a member of the superfamily of multi-copper oxidases (E.C. 1.10.3.2). First discovered in extracts from the Chinese lacquer tree (*Toxicodendron vernicifluum*, previously named *Rhus vernicifera*), laccases have since been found in a variety of organisms including plants, fungi, bacteria, and archaea.[39−42] Laccases utilize a multi-copper cofactor for substrate oxidation.[43] Rather than requiring H_2O_2 as in other lignolytic enzymes, laccases use O_2 as the final electron acceptors.[44−46] Furthermore, oxidation of small-molecule mediators by laccase, such as 1-hydroxybenzotriazole (HBT) or 2,2′-azino-bis(3-ethylbenzothiazoline-6-sulfonic acid) (ABTS), enables the oxidation of nonphenolic lignin compounds.[47,48] This feature, alongside their inherent lignolytic capabilities and their activity under milder reaction conditions, makes laccases a desirable biocatalyst for lignin upgrading strategies.[49,50] ILs have been found to be capable of supporting and, in a few cases, improving activity and stability of enzymes including laccases.[51−54] *Trametes versicolor* laccase (*TvL*) activity decreased with increasing IL concentration of the two alkylimidazolium ILs tested, $[C_2C_1Im][EtSO_4]$ and $[C_2C_1Im][OAc]$.[55] However, Galai et al. screened *TvL* activity in 56 AILs and found that 13 of the AILs improved laccase activity; the most notable improvement was seen in choline dihydrogenphosphate ($[Ch][H_2PO_4]$) which increased laccase activity by 451%.[56]

Given the unique properties that certain AILs provide regarding lignin solubility and biocompatibility, the confluent utilization of AIL and LDEs holds great potential for developing a new strategy for lignin extraction and depolymerization. Despite previous exploration of biocatalysis and enzyme activity in AILs, there is a gap in our understanding of the mechanisms underlying the interactions between lignolytic enzymes and these solvents. This study aims to elucidate the interactions between laccase and ILs, inhibition mechanism and product profiling on such a biocatalytic system with laccase and three AILs. To achieve this goal, we screened the ILs 1-ethyl-3-methylimidazolium acetate ($[C_2C_1Im][OAc]$), [Ch][Lys], and diethylamine hydrogensulfate ($[DEA][HSO_4]$) for their biocompatibility with a fungal laccase. We then investigated enzyme kinetics and the inhibition mechanism using docking simulations with the ILs and the active site. Finally, the IL−laccase system was tested on a β-O-4′ linked model dimer [guaiacylglycerol-β-guaiacyl ether (GGE)] and commercial kraft lignin in the presence of the mediator, ABTS; the resulting residual lignin and lignin-derived products were then characterized. This work provides a better understanding of the inhibition mechanisms of ILs on laccase for developing a biocatalytic lignin valorization process using AILs and LDEs.

METHODS AND MATERIALS

Materials. Laccase from *T. versicolor* (0.66 U/mg), ABTS, alkaline lignin (lot# MKBV5831V), choline hydroxide, L-lysine, and the IL $[C_2C_1Im][OAc]$ were purchased from MilliporeSigma (St. Louis, MO, USA). Diethylamine (DEA), sulfuric acid (H_2SO_4), GGE, tetrahydrofuran (THF), 2-methyltetrahydrofuran (MeTHF), chromium(III)acetylacetonate ($Cr(acac)_3$), and ethyl acetate were purchased from Tokyo Chemical Industry Co. (Portland, OR, USA). The ILs, [Ch][Lys], and $[DEA][HSO_4]$ were synthesized using the anion and cation precursors according to previously developed protocols.[36]

Biocompatibility Screening. The biocompatibility of the three ILs, $[C_2C_1Im][OAc]$, [Ch][Lys], and $[DEA][HSO_4]$ in their aqueous solution (approximate 1−10% w/v), was screened with *TvL*. To delineate the effect of pH, the IL solutions were adjusted to pH 5.0 using 1 M sodium hydroxide or 1 M hydrochloric acid prior to testing. Activity was screened with 20 mM sodium citrate buffer, AIL (0, 1, 2, 3, 4, or 10% w/v), and 2 mM ABTS in clear, flat bottom 96-well Costar assay plates (Corning Inc., Kennebunk, ME). Laccase was loaded at 3 concentrations: low (0.6 μg mL^{-1}), medium (1.2 μg mL^{-1}), and high (3.0 μg mL^{-1}). The plate was incubated at 40 °C in a SpectraMax M2 plate reader (Molecular Devices, Sunnyvale, CA). Absorbance readings were taken every 30 s for 5 min at a wavelength of 420 nm. Plates were shaken for 5 s prior to initial reading and 3 s before each reading to ensure well mixing. Oxidation of ABTS in buffer and AILs without laccase were measured as blanks.

Inhibition Kinetics. Michaelis−Menten curves were generated for different IL concentrations by measuring initial velocities for 11 different ABTS concentrations at a medium loading (1.2 μg mL^{-1}) of laccase. ABTS oxidation was measured using the same method as described in the biocompatibility screening in 96-well plates. The oxidized ABTS was quantified using an absorbance coefficient, ε = 36 000 M^{-1} cm^{-1}.[57] A unit of activity was defined as the amount of laccase that oxidizes 1 μmol of ABTS per min. Laccase initial activity as a function of ABTS concentration ([S]) was fit to the Michaelis−Menten curve, shown in eq 1.

$$V = \frac{V_{max} \times [S]}{K_m + [S]} \quad (1)$$

These curves were linearized using the Hanes−Woolf method, resulting in eq 2.

DOI: 10.1021/acssuschemeng.9b02151
ACS Sustainable Chem. Eng. 2019, 7, 15928−15938

$$\frac{[S]}{V} = \frac{1}{V_{max}} \times [S] + \frac{K_m}{V_{max}} \quad (2)$$

Equation 2 was used to calculate the kinetic coefficients, K_m and V_{max} of laccase in different AILs.

Molecular Docking Simulations. In order to determine likely interactions between IL molecules and laccase, docking simulations were performed using the YASARA Structure software package (YASARA Biosciences GmbH, Vienna, Austria) with the AutoDock Vina plugin.[58] Ion structures and parameters were generated in YASARA from SMILES representations and energy minimized. The crystal structure of *TvL* (PDB ID: 1GYC) was used as a target in the docking simulations.[43] Cations and anions were treated as separate ligands, with 25 simulations run for each, and the target laccase was held rigid throughout all simulations. Results of docking were visualized with PyMol (Schrodinger LLC, New York, NY).

Lignin Depolymerization in AIL. *GGE Dimer.* Prior to experiments with the model compound, all solutions were adjusted to pH 5.0 with 1 M sodium hydroxide or 1 M hydrochloric acid. Laccase was loaded to a final concentration of 1.2 μg mL^{-1} and ABTS was added for a final concentration of 2 mM. The GGE model compound was added for a final concentration of 0.5 mg mL^{-1}. AILs were added for final concentrations of 2% (w/v) [C_2C_1Im][OAc], 1% [Ch][Lys], and 10% [DEA][HSO_4]. Reactions were carried out in 1 mL glass tubes under 30 psi O_2 pressure at 40 °C inside a 100 mL Parr reactor (4593 bench top reactor, Alloy C276, Parr Instruments, IL). The reactor was purged with pure O_2 for 1 min and then the release valve was closed to maintain O_2 pressure. The reaction was allowed to proceed for an additional 2 h.

After reaction, product profiles were analyzed by isocratic high-performance liquid chromatography (HPLC) using an 80% water−20% acetonitrile mobile phase at a flow of 0.5 mL min^{-1} for 30 min through an Ultimate 3000 HPLC system (Dionex Corporation, Sunnyvale, CA) equipped with an ultraviolet (UV) detector. Separation was achieved through the use of a ZORBAX Eclipse XDB-C18 column (5 μm particle size, 150 × 4.6 mm i.d., Agilent Technologies, Santa Clara, CA) at 25 °C. Elution profiles were measured by UV absorbance at 280 nm. The molecule weight distribution of the products was characterized using gel permeation chromatography (GPC), whereas liquid chromatography−mass spectrometry (LC−MS) was used to identify the major products in GGE experiment as described in the "Lignin Characterization" section.

Alkaline Lignin. The same reaction protocol was used for alkaline lignin samples as for the GGE dimer except that 500 mg of kraft lignin was loaded with the reactants (1.2 μg mL^{-1} laccase, 2 mM ABTS, AILS) in the Parr reactor with a final reaction volume of 10 mL. After the reaction, residual lignin was precipitated by addition of 20 mL water and centrifugation at 7000 rpm for 15 min. The aqueous fraction was subjected to liquid−liquid extraction using a 1:1 volume of ethyl acetate: liquid fraction, with the extraction repeated 3 times. The ethyl acetate was evaporated in a vacuum oven set at room temperature for 24 h to leave a thick oil. Oil yield was calculated using eq 3.

$$\text{Oil yield (\% yield)} = \frac{\text{weight of oil}}{\text{weight of initial lignin}} \times 100 \quad (3)$$

The precipitated solids (residual lignin) were washed with 50 mL water three times to remove any excess IL and dried in a convection oven at 45 °C for 48 h. Lignin conversion was calculated using eq 4.

$$\text{Conversion (\%)} = \frac{\text{weight of initial lignin} - \text{weight of remaining lignin}}{\text{weight of initial lignin}} \times 100 \quad (4)$$

The oil was dissolved in 750 μL MeTHF and analyzed by gas chromatography (GC)−MS for lignin decomposition products. Identification and quantification of the monomeric products from the depolymerization reaction were performed on an Agilent 7890B GC coupled to a 5977B MS with an HP-5ms (60 m × 0.32 mm) capillary column.[59] The temperature program started at 50 °C and increased to 120 °C at 10 °C min^{-1} with a holding time of 5 min; then it was raised to 280 °C at 10 °C min^{-1} with a holding time of 8 min and to 300 °C at 10 °C min^{-1} with holding time of 2 min.[60] The inlet was held in the splitless mode at 250 °C using helium as a carrier gas at a flow rate of 1.2 mL min^{-1}. Calibration curves were created using commercially available pure compounds: guaiacol, syringol, vanillin, acetovanillone, and homovanillic acid (Sigma-Aldrich, St. Louis, MO). Monomer yields were calculated on the basis of mg/g starting lignin.

Lignin Characterization. *Gel Permeation Chromatography.* The weight-average molecular weight (M_w) and number-average molecular weight (M_n) of both precipitated lignin and lignin products in the liquid phase following the reactions were determined by GPC. The precipitated lignin was acetylated via acetobromination.[61] In brief, 10 mg of the lignin was dissolved in 2.5 mL of 92:8 (v/v) acetic acid and acetyl bromide and mixed at 50 °C for 2 h. Excess acetic acid and acetyl bromide was evaporated by purging with N_2. The acetylated lignin was dissolved in 750 μL of THF and analyzed by direct injection into an HPLC system equipped with a Mixed-D PLgel column (5 μm particle size, 300 × 7.5 mm i.d., molecular weight range of 200−400 000 μm, Polymer Laboratories, Amherst, MA, USA) at 50 °C. The THF flow rate was 0.5 mL min^{-1}. Eluted molecular species were detected by absorbance at 300 nm, which was calibrated using a polystyrene standards kit (Sigma-Aldrich, St. Louis, MO). The molecular weight distribution of model compound products was analyzed by direct injection into the HPLC system using the aforementioned method.

Fourier Transform Infrared Spectroscopy. Chemical structures of alkaline lignin and treated lignin were determined using a Thermo Nicolet 870 FTIR-ATR spectrometer. Lignin sample spectra were obtained with 64 scans at wavelengths from 700 to 4000 cm^{-1} with a spectral resolution of 2 cm^{-1}. The raw Fourier transform infrared spectroscopy (FTIR) spectra were baseline corrected and normalized using Omnic 6.1a software and compared in the range 750−4000 cm^{-1}.

Differential Scanning Calorimetry. Differential scanning calorimetry (DSC) measurements of alkaline and treated lignin samples were performed using a DSC Q20 (TA Instruments, New Castle, DE) equipped with an autosampler. Analysis was carried out in a temperature range of 40−500 °C at a rate of 10 °C min^{-1} and N_2 flow of 50 mL min^{-1}.

^{1}H−^{13}C HSQC NMR. Approximately 100 mg of the lignin sample along with ca. 1 mg of Cr(acac)$_3$ were dissolved in DMSO-d_6/pyridine-d_5 (4:1) under mild heat and sonication in a NMR tube until a homogeneous mixture was obtained. NMR spectra were acquired on a 500 MHz JEOL ECZr (Peabody, MA, USA) spectrometer equipped with a 5 mm Royal Probe. The central DMSO solvent peak was used as an internal reference (δ_C 39.5, δ_H 2.5 ppm). The ^{1}H−^{13}C correlation experiment was a heteronuclear single quantum coherence (HSQC) experiment (JEOL standard pulse sequence "hsqc_dec_-club_pn"). HSQC experiments were carried out using the following parameters: acquired from 12 to 0 ppm in f2 (^{1}H) with 1024 data points (acquisition time 136 ms), 220 to 0 ppm in f1 (^{13}C) with 256 increments, and 150 scans with a 1 s interscan delay. In all cases, processing used typical sine bell (90°) in f2 and squared sine-bell (90°) in f1 (first point 0.5). Volume integration of contours in HSQC plots used Mestrelab MestReNova 12.0 (Mac version) software. Integrals were from volume-integration of C/H pairs with similar properties, the α-C/H correlations of A (β-O-4′), B (β–β′), and C (β-5) units. Spectra are displayed in the absolute value mode and color coded (in Adobe Illustrator CC 2018) using the literature reference standards.[62]

Model Compound MS. MS, to identify large molecular weight products from GGE experiments, was performed on a Q-Exactive (Thermo Scientific, Waltham, MA, USA) orbitrap spectrometer. The instrument parameters were as follows: a 3.8 kV spray voltage, 225 °C inlet temperature, sheath auxiliary gas flow of 2 (arbitrary units), a mass resolution of 140 000, with nitrogen as the HCD collision gas. A

DOI: 10.1021/acssuschemeng.9b02151
ACS Sustainable Chem. Eng. 2019, 7, 15928−15938

10 μL aliquot of each sample was reduced to dryness under nitrogen. The dry residue was dissolved in 100 μL of a solution containing 50% acetonitrile and 50% 10 mM aqueous sodium hydroxide. The final solution was infused directly into the mass spectrometer by syringe pump at a flow rate of 3 mL per min. For the HCD tandem MS experiments, precursor ions were isolated using a window of 3 m/z, and a normalized collision energy of 25 NCE was applied. Data were processed using Xcalibur software (Thermo Scientific, Waltham, MA, USA).

RESULTS AND DISCUSSION

Biocompatibility Screening. In order to test whether laccase is still active in AIL solution, three ILs were screened for their biocompatibility with *TvL* at concentrations ranging from 1 to 10% IL in water. Results indicate that [Ch][Lys] and [C_2C_1Im][OAc] are more inhibitory to *TvL* with 2% [Ch][Lys] or 5% [C_2C_1Im][OAc] causing significant loss (>70%) of *TvL* activity (Figure 1). In contrast, [DEA][HSO_4] is more compatible with *TvL*, as indicated by the modest loss (<20%) of *TvL* activity even at 10% concentration. The tested IL concentrations represented a reported range of AIL biomass pretreatment conditions. For example, Liu et al. showed that 10% [Ch][Lys] was highly effective in removing lignin from switchgrass varieties during pretreatment,[63] and [C_2C_1Im][OAc] at 20−50% in water can remove a large portion of the hemicellulose and lignin when compared to pure IL.[64,65] Gschwend et al. have demonstrated that 80 wt % triethylammonium hydrogen sulfate ([TEA][HSO_4]) is capable of improving *Miscanthus* saccharification yields and lignin removal after pretreatment for 15 min at 180 °C.[66]

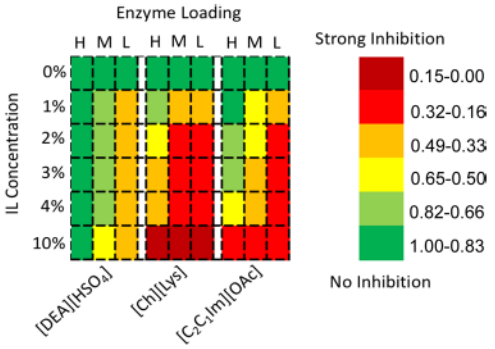

Figure 1. Activity of *TvL* in AIL solutions. H = high laccase concentration (3.0 μg mL^{-1}), M = medium laccase concentration (1.2 μg mL^{-1}), L = low laccase concentration (0.6 μg mL^{-1}). Values indicate the ratio of *TvL* activity in ILs relative to *TvL* activity in buffer (0% IL).

Both the cations and anions of the AILs could impact their activity. It has been shown that the toxicity of imidazolium-based ILs increases with increasing cation size.[67] [C_2C_1Im][OAc] at 2% concentration strongly inhibited cellulase activities and growth of common biofuel fermentation microbes such as yeast and *Escherichia coli*,[68] whereas [Ch][Lys] exhibited low toxicity to yeast and *E. coli*.[69] A more recent study further suggested that cellulase enzymes and yeast can tolerate 5% [Ch][Lys].[70] However, it appeared that [Ch][Lys] was more inhibitory to the *TvL* than [C_2C_1Im][OAc] and [DEA][HSO_4]. This case agrees with previous reports showing that ILs with sulfate anions are generally more biocompatible with laccases.[71,72] However, we did not control for the cation between each AIL, so the biocompatibility cannot be solely attributed to the anion in this case.

Inhibition Mechanisms. To better understand the different effects of the three ILs on *TvL*, we determined their inhibition kinetics using ABTS as a substrate. [C_2C_1Im][OAc] and [Ch][Lys] are mixed inhibitors of *TvL*, decreasing V_{max} and increasing K_m (Table 1). This type of inhibition suggests that the ILs do not directly compete with the substrate for the active site, but rather affect the residues surrounding the active site to interfere with substrate binding. [DEA][HSO_4] in contrast is a noncompetitive inhibitor, not affecting substrate binding but decreasing the catalytic rate of the enzyme. To the best of our knowledge, there have not been any previous studies assessing the inhibitory mechanisms of [Ch][Lys] and [DEA][HSO_4] on laccases. The effects of alkylimidazolium ILs on *TvL* kinetics have been reported, although no studies have been performed with [C_2C_1Im][OAc]. Tavares et al. found that three ILs with a [C_2C_1Im]$^+$ cation reduced both the V_{max} and K_m of *TvL* with ABTS as a substrate, supporting our finding with [C_2C_1Im][OAc].[73]

Table 1. Kinetic Constants of ABTS Oxidation by *TvL* in AILs[a]

IL	IL concentration 0% (w/w)	2% (w/w)	5% (w/w)
	V_{max} (U/mg *TvL*)		
[C_2C_1Im][OAc]	23.1 ± 1.0[a]	16.2 ± 2.4[b]	9.0 ± 0.4[c]
[Ch][Lys]	23.1 ± 1.0[a]	7.2 ± 0.3[b]	5.8 ± 0.3[b]
[DEA][HSO_4]	23.1 ± 1.0[a]	17.9 ± 0.3[b]	21.6 ± 0.3[a]
	K_m (mM ABTS)		
[C_2C_1Im][OAc]	0.065 ± 0.023[a]	0.531 ± 0.090[b]	1.469 ± 0.012[c]
[Ch][Lys]	0.065 ± 0.023[a]	1.154 ± 0.124[b]	2.847 ± 0.300[c]
[DEA][HSO_4]	0.065 ± 0.023[a]	0.104 ± 0.013[a]	0.111 ± 0.023[a]

[a]The superscript letters "abc" indicate the significance levels of the means.

Docking Simulations. To gain a deeper insight into the inhibition mechanisms, docking simulations were carried out with the IL cations and anions (Figure 2). A high probability binding site for [C_2C_1Im][OAc] and [Ch][Lys] was found near the type I copper, thus possibly decreasing the catalytic rate by obstructing removal of electrons during substrate oxidation at the type I copper. Binding of these ILs at this site may also interfere with ABTS interaction, accounting for the observed increase in K_m. In contrast, a binding site for [DEA][HSO_4] was not identified with any significant probability near the active site, which is consistent with the observed weak noncompetitive inhibition.

Docking simulation of [C_2C_1Im][OAc] in this study corroborates a previous study on alkylimidazolium ILs and laccases. Molecular dynamics simulations with alkylimidazolium cations found that cations of varying chain length interacted with the active site via hydrophobic interactions.[74] The shorter chain length cations (C_2−C_6) were capable of diffusing into the active site; longer chain length cations (C_8−C_{10}) were limited to binding to Leu residues around the active-site entrance. Several studies have shown that enzyme−IL interactions, particularly interactions with the anions, lead to disruption of protein stability as predicted by the Hofmeister series.[30,75,76] The more chaotropic anions lead to disruption of the water shell around a protein, causing destabilization of the protein. The specific anion effect can only be assessed when

DOI: 10.1021/acssuschemeng.9b02151
ACS Sustainable Chem. Eng. 2019, 7, 15928−15938

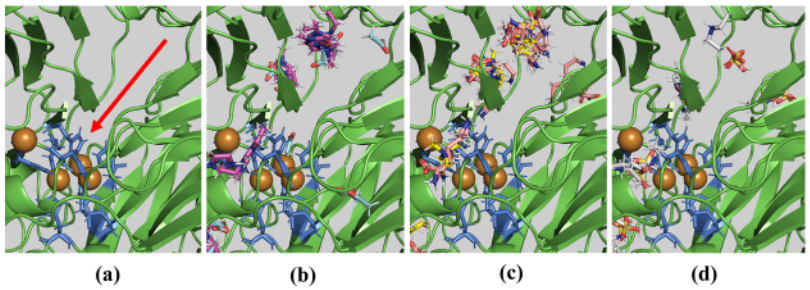

Figure 2. Results of simulations showing the docking of (b) [C_2C_1Im][OAc], (c) [Ch][Lys], and (d) [DEA][HSO_4] near the type I copper of *TvL*. The red arrow in (a) points to the type I copper. The ILs are represented by the multicolored stick models in panels (b–d) and the His residues that coordinate the coppers are colored blue.

the cation is consistent, but $[HSO_4]^-$ has been observed to be among the most stabilizing of the anions.[77]

GGE Dimer Transformation. The activity screening results support the possibility of using *TvL* in dilute or more concentrated AIL solutions, depending on the IL introduced, to process lignin. The phenolic lignin dimer (GGE) was first tested because the dimer is linked by β-O-4′ bond, which is the most common interunit linkage in lignin. In absence of ABTS, *TvL* in 1% [Ch][Lys] or 2% [C_2C_1Im][OAc] was inhibited from processing GGE, whereas *TvL* in 10% [DEA][HSO_4] experiences no inhibition to processing GGE (Figure 3a). Some studies have found that acidic ILs are capable of cleaving the β-O-4′ linkage on their own at elevated temperatures.[78] The temperature used in this study (40 °C) was much lower than previous studies (150 °C), so it is unlikely that the [DEA][HSO_4] itself was responsible for any major changes made to GGE during the reaction. Upon addition of ABTS, *TvL* is able to process GGE in the presence of all ILs (Figure 3b).

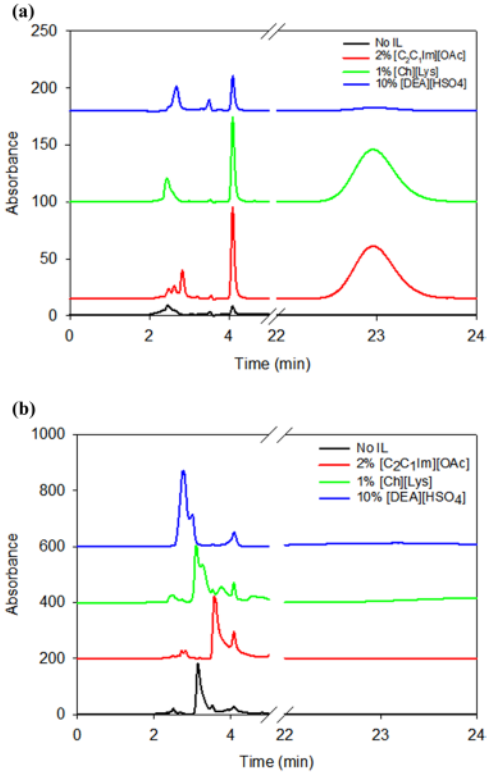

Figure 3. HPLC chromatograms of GGE incubated with laccase and different AILs (a) without ABTS present during the reaction. (b) ABTS present during the reaction. GGE elutes at ~23 min and reaction products elute in the 2–5 min range.

To better assess changes made to GGE during the reaction, the products were further analyzed with GPC and LC–MS. The weight-average molecular weight (M_w), number-average molecular weight (M_n), and the polydispersity index (PDI) of all samples increased during the reaction with GGE (Table 2).

Table 2. Molecular Weight Distribution of GGE before (0 min), during (30 min), and after (120 min) Treatment with *TvL*, ABTS, and ILs[a]

IL	0 min	30 min	120 min
	M_w (g mol^{-1})		
no IL	447	941	1315
2% [C_2C_1Im][OAc]	447	877	975
1% [Ch][Lys]	447	881	1087
10% [DEA][HSO_4]	447	993	984
	M_n (g mol^{-1})		
no IL	402	817	1118
2% [C_2C_1Im][OAc]	402	742	576
1% [Ch][Lys]	402	741	694
10% [DEA][HSO_4]	402	762	519
	PDI		
no IL	1.11	1.15	1.18
2% [C_2C_1Im][OAc]	1.11	1.18	1.69
1% [Ch][Lys]	1.11	1.19	1.57
10% [DEA][HSO_4]	1.11	1.30	1.90

[a]M_w: weight-average molecular weight, M_n: number-average molecular weight, PDI: polydispersity index.

The samples with an IL present had a lower M_w and higher PDI after 120 min compared to the control without AIL. The M_w of the control after 120 min was 1315 g mol^{-1}, whereas the highest M_w of samples with IL was 1087 g mol^{-1} in 1% [Ch][Lys]. The PDI of the No IL control was 1.18 after 120 min, whereas the PDI of samples with ILs were 1.57 (1% [Ch][Lys]), 1.69 (2% [C_2C_1Im][OAc]), and 1.90 (10% [DEA][HSO_4]). The M_n of IL samples decreased between 30 and 120 min, which led to the substantial increase in PDI at the end of the reaction. Molecular weight distribution plots (Figure 4) suggest this is a result of low-molecular weight species appearing in the 120 min samples. To identify any higher-order structures, for example dimers, trimers, or oligomers, extracted products were identified with LC–MS.

Direct infusion MS experiments using a high-resolution accurate-mass orbitrap mass spectrometer (Q-Exactive) (Thermo Scientific, Waltham, MA, USA) in the negative ion

DOI: 10.1021/acssuschemeng.9b02151
ACS Sustainable Chem. Eng. 2019, 7, 15928–15938

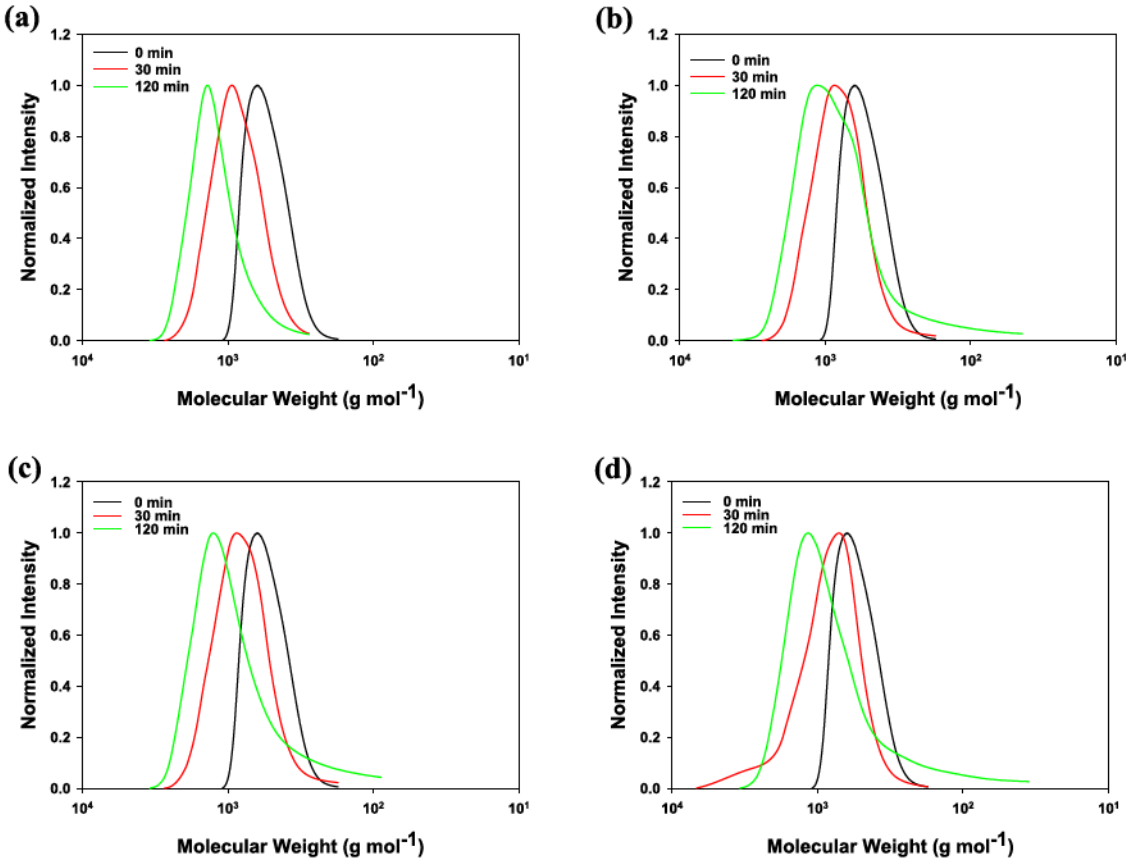

Figure 4. Molecular weight distributions of products after GGE reaction with *TvL*, ABTS, and (a) buffer without IL, (b) 2% $[C_2C_1Im][OAc]$, (c) 1% [Ch][Lys], (d) 10% $[DEA][HSO_4]$.

Table 3. Conversion and Yield of Alkaline Lignin Degradation Products

			identifiable monomer yield (% of starting lignin)				
sample	conversion (%)	lignin oil yield[a] (%)	guaiacol	vanillin	syringaldehyde	acetovanillone	total
no IL	2.12	0.74	0.000	0.102	0.059	0.046	0.207
2% $[C_2C_1Im][OAc]$	11.72	0.84	0.000	0.115	0.068	0.054	0.237
1% [Ch][Lys]	17.24	1.28	0.054	0.186	0.124	0.098	0.462
10% $[DEA][HSO_4]$	21.66	0.74	0.018	0.145	0.081	0.068	0.312

[a]Fractions extracted using ethyl acetate.

mode with sodium hydroxide as a pH modifier were performed. The infusion mass spectra were dominated by three ion peaks with m/z values much greater than those for the starting GGE dimer. High-resolution, accurate mass spectra and tandem MS allowed the probable identity of these species to be defined. The ion peak at m/z 637.1919 was consistent with the coupling of two GGE dimers (GGE dimer MW 320 g mol^{-1}) with the proposed structure shown in Figure S2a (calculated m/z 637.1927, observed m/z 637.1918, error 1.3037 ppm). The ion peak at m/z 953.3242 was consistent with the coupling of three GGE dimers with the proposed structure shown in Figure S2b (calculated m/z 953.3237, observed m/z 953.3241, error 0.3765 ppm). Finally, the ion peak at m/z 1073.3454 was consistent with the addition of a G monomer unit to the three GGE oligomers (m/z 953.3242) with the proposed structure shown in Figure S2c (calculated m/z 1073.3449, observed m/z 1073.3448, error −0.0172 ppm).

Previous studies have shown that laccases facilitate both the depolymerization and polymerization of lignin model compounds. LC−MS analysis of extracted products formed during guaiacylic and syringilic lignin model compound oxidation by *Melanocarpus albomyces* and *Trametes hirsuta* laccases showed that GGE homodimerized to form a single product via a 5−5′ coupling mechanism, which is identical to that shown in Figure S2a.[79] ABTS was also found to participate in the polymerization of a β-O-4′ lignin model dimer and guaiacol when treated with *T. hirsuta* laccase, although the structures of the products formed during the reaction were not identified.[80] Neither of these studies investigated the role of ILs during polymerization of lignin model compounds. We have shown that the presence of ABTS and, possibly the ILs, facilitates the polymerization of GGE into structures larger than the single GGE homodimer reported previously.[79] Additionally, the molecular weight distributions of the reaction products suggest that the presence of ILs promotes the formation of low-molecular weight compounds during model compound polymerization/depolymerization.

Depolymerization of Alkaline Lignin. To further investigate the utility of *TvL*−AIL systems, we tested their

DOI: 10.1021/acssuschemeng.9b02151
ACS Sustainable Chem. Eng. 2019, 7, 15928−15938

ability to depolymerize commercial alkaline lignin with the same reactors used for other studies. In comparison to a control lacking IL (2.12% conversion based on the mass of residual solids), higher lignin conversions were achieved for *TvL* catalysis of alkaline lignin in AIL systems (Table 3). The highest conversion was obtained with *TvL* in 10% [DEA][HSO_4] (21.66%), followed by *TvL* in 1% [Ch][Lys] (17.24%) and *TvL* in 2% [C_2C_1Im][OAc] (11.72%). However, 1% [Ch][Lys] resulted in the highest yield of oil (1.28%) as compared to 2% [C_2C_1Im][OAc] (0.84%) and 10% [DEA][HSO_4] (0.74%). Analysis of extracted products with GC−MS revealed vanillin to be the primary degradation product (consisting 55−70% of the quantifiable monomers), followed by syringaldehyde, acetovanillone, and guaiacol (Figure 5).

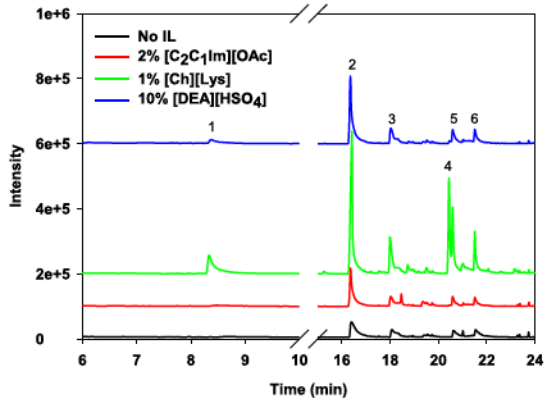

Figure 5. GC−MS chromatograms of alkaline lignin breakdown products after treatment with laccase, AILs, and ABTS. Major products identified were (1) guaiacol, (2) vanillin, (3) acetovanillone, (4) homovanillic acid, (5) syringaldehyde, and (6) acetosyringone.

The discrepancy between lignin conversion and oil yield, which was particularly marked for [DEA][HSO_4] (21.66% conversion vs 0.74% oil yield), could be attributed to less extractable oligomeric compounds formed by the laccase, similar to the condensation of the GGE model compound, which cannot be detected by GC−MS.

GPC results revealed that all treatments led to a small increase in average molecular weight when compared to untreated alkaline lignin (Table 4). Additionally, the PDI decreased for all treatments when compared to untreated alkaline lignin. Treatment of alkaline lignin with laccase and 1-hydroxybenzotriazole (HBT), another mediator, resulted in a reduced PDI and increased molecular weight.[81] GPC of supernatants revealed the presence of higher molecular weight solids in treatments with ILs compared to treatment without IL. These results indicate that the laccase−AIL system could facilitate both depolymerization of lignin to a low molecular weight fraction as well as larger products resulting from subsequent polymerization. This polymerization could be limited by a capping agent such as phenol, which has been used to improve monomer yields from organosolv olive tree pruning lignin,[82] although the amount of phenol required is quite high (2:1 phenol/lignin). The results with the model compound suggest that some AILs could act as biocompatible capping agents, although this possibility will need to be investigated further in a separate study.

The chemical and structural properties of the resulting lignin stream were further characterized using FTIR, DSC, and 2D HSQC NMR. Analysis of FTIR spectra indicated minimal differences between untreated and treated lignin samples (Figure S3a). The only difference can be seen is in the peak at 1110 cm^{-1}. This peak corresponds to the aromatic C−H plane deformation in S-lignin and is reduced for treated lignin samples when compared to untreated alkaline lignin, which is consistent with the identification of derivatives of S-lignin with GC−MS. The bands at 1220 cm^{-1} corresponding to C−C, C−O, and C=C stretching in G-lignin were unchanged for treated lignin when compared to untreated alkaline lignin. Preferential breakdown of S-lignin has been observed before via oxidation of alkaline lignin using transition-metal catalysts, so its possible that the biocatalyst follows the same trend.[37,83] Thermal profiles as shown by DSC are similar for all samples of untreated and treated alkaline lignin (Figure S3b). Exothermic and endothermic regions are indicated by positive and negative values of H_β respectively. An exothermic region between 50 and 100 °C was observed for all samples. Similarly, an endothermic region between 400 and 450 °C was observed for all samples. The mild reaction conditions, relatively low temperature, and low IL concentrations did not appear to result in any significant changes to the lignin structure.

2D HSQC NMR spectra show a small amount of S-lignin in the starting material, however, there does not appear to be a substantial reduction in these peaks after processing, suggesting that only a small portion of the starting material was solubilized during processing (Figure 6). There appears to be shifts in the ratios of β-O-4′ and β−β′ linkages in alkaline lignin after treatment, but these changes are not above experimental variation. The most substantial changes were the relative ratios of β-O-4′ and β−β′ linkages in the alkaline lignin treated with laccase and ABTS (KLA), whereas alkaline lignin treated with laccase and ABTS in [C_2C_1Im][OAc] (EKLA) saw relatively minor changes in the HSQC. β-O-4′ linkages in alkaline lignin treated without any AILs present were reduced from 54 to 41%. Alkaline lignin treated with aqueous [C_2C_1Im][OAc] in addition to laccase and ABTS resulted in increased β-O-4′ (54% → 56%) and reduced β−β′ (29% → 26%) linkages. Previously, Li et al., reported that the water-insoluble fraction of alkaline lignin after treatment with laccase and the mediator

Table 4. Processed Lignin Molecular Weight Distribution and Polydispersity of Lignin Streams[a]

	solid phase			liquid phase		
sample	M_w (g mol^{-1})	M_n (g mol^{-1})	PDI	M_w (g mol^{-1})	M_n (g mol^{-1})	PDI
alkaline lignin	5677	1974	2.88	N/A	N/A	N/A
no IL	5457	2470	2.21	693	450	1.54
2% [C_2C_1Im][OAc]	5358	2482	2.16	709	542	1.31
1% [Ch][Lys]	5772	2454	2.35	654	535	1.22
10% [DEA][HSO_4]	6170	2068	2.98	667	526	1.27

[a]M_w: weight average molecular weight; M_n: number average molecular weight; PDI: polydispersity index; N/A: not applicable.

DOI: 10.1021/acssuschemeng.9b02151
ACS Sustainable Chem. Eng. 2019, 7, 15928−15938

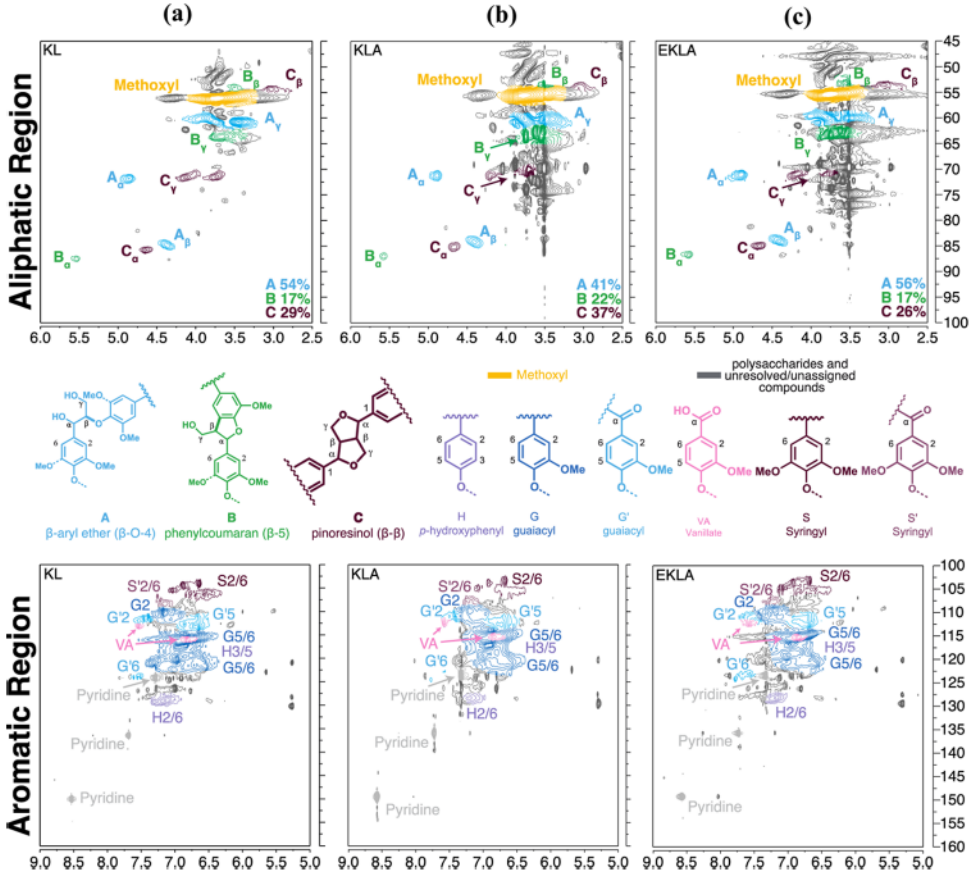

Figure 6. $^{13}C-^{1}H$ (HSQC) spectra of aliphatic (top) and aromatic (bottom) regions of (a) raw alkaline lignin (KL), (b) alkaline lignin treated with laccase and ABTS in buffer (KLA), and (c) alkaline lignin treated with laccase and ABTS in 2% $[C_2C_1Im][OAc]$ (EKLA). Figure S6 in the Supporting Information contains all of the spectra from the study. The structures of side-chain linkages and lignin compositional units, shown in the middle of the figure, were coded with colors corresponding to the cross peaks in the spectra aliphatic and aromatic regions, respectively. Linkage percentages were calculated via volume integration of the $C_\alpha-H$ of the β-O-4′, β-5′, and $\beta-\beta'$ linkages and treated as a relative ratio of the three. Volume integrations are intended to be only semiquantitative due to problems inherent to HSQC experiments including a wide array of potential $^{1}J_{C-H}$ values and rates of T_2 relaxation.[59]

HBT had increased the β-O-4′ (61.5% → 68.5%) and reduced $\beta-\beta'$ (5.8% → 5.7%) content compared to the starting material, suggesting the presence of less branched lignin structure when compared to the starting material.[81]

It is possible that there are IL-specific effects that altered the changes in linkage ratios seen after treatment with laccase and ABTS. The relative content of ether bond was based on NMR analysis of the residual solids rather than the liquid products. Results suggest that the relative ether bond content stayed unchanged or slightly increased in the residual solids. The relatively small increase in ether bonds from KLA to EKLA is likely negligible, however, it is possible that dehydrogenation reactions of the $\beta-\beta$ linkages rendered a small amount of these linkages without C−H groups at the $C_\alpha-H$ and $C_\beta-H$ positions causing a small increase in the β-O-4 content. A similar phenomenon has been observed when kraft lignin was treated with *TvL* and 1-hydroxybenzotriazole hydrate (HBT), which is another mediator.[81] The insoluble lignin fraction in the study had a higher ether bond content than the starting material. It is also noted that these numbers should not be over-interpreted as HSQC NMR is a semi-quantitative method (because of variations in T_2 relaxations and $^{1}J_{C-H}$ constants) for quantifying the linkages in their relative ratios. It is surprising that S-lignin was identified in the raw and treated kraft lignin samples. We encountered the similar problem in our previous work[38] where a small quantity of S-lignin was observed in the original Sigma-Aldrich alkaline lignin. Although the majority of the lignin is likely softwood, it is possible that the lignin streams used for the Sigma-Aldrich kraft lignin are made of a small amount of other species (e.g., hardwood).

The source of the lignin itself could play a role in the depolymerization because the alkaline (kraft) lignin has been reported to be heterogeneous and condensed.[84] To fully understand these effects, a less recalcitrant lignin source may be tested as the commercial alkaline/kraft lignin tends to be more condensed (more C−C bonds) than the native lignin in plants.[85] Because of the intrinsic complexity of real lignin (alkaline lignin in this study) and the limitations of current lignin analytical approaches, many of the proposed lignin transformation mechanisms are based on lignin model compounds such as monolignols and GGE dimmer. In this work, we were able to identify the major products in the GGE experiment using LC−MS and propose possible reaction pathways. The lignin transformation mechanism with the GGE dimmer could be partially transferable to the alkaline lignin substrate; however, to fully reveal the alkaline lignin transformation mechanism is still very challenging based on current lignin analytical techniques.

DOI: 10.1021/acssuschemeng.9b02151
ACS Sustainable Chem. Eng. 2019, 7, 15928−15938

Summarizing the results of GGE dimer and alkaline lignin depolymerization, it was found that *TvL* in aqueous $[C_2C_1Im][OAc]$ and [Ch][Lys] require the presence of the mediator ABTS to process the β-O-4′ lignin model compound. Alternatively, *TvL* in $[DEA][HSO_4]$ does not require ABTS to process with the compound. GPC and LC−MS analysis of the reaction products indicates that GGE was initially polymerized into dimers, trimers, and oligomers of the model compound. As the reaction proceeded, the ILs limited this polymerization and appeared to promote the formation of small-molecular weight products. *TvL* in AIL promoted both the depolymerization and polymerization of the alkaline lignin, and the improved monomer yield could be attributed to the cleavage of the β-O-4′ linkages. Obtaining high lignin monomer yield is important from lignin valorization standpoint. As the main focus of our study is to understand the interactions among lignolytic enzymes, lignin, and IL solvents, we were not set to optimize lignin depolymerization; indeed, we picked relatively mild reaction conditions to better probe the initial stage of the reaction and catch the product profile. Further optimizing the reaction conditions would likely improve the yield of aromatic monomers from enzymatic lignin depolymerization. Native plant lignin can be used as a substrate in future studies, in place of the highly condensed kraft lignin used in this study. Additionally, other laccases or laccase-engineering strategies can be employed to develop a biocatalyst with resistance to higher IL concentrations or operating temperatures.

CONCLUSIONS

This study provides insight into the interactions between *TvL* and AILs. The effects of three AILs with distinct properties on *TvL* activity, inhibition mechanism, and oxidative capability were investigated. Results indicate that $[DEA][HSO_4]$ did not impede the ability of *TvL* to oxidize ABTS, whereas $[C_2C_1Im][OAc]$ and [Ch][Lys] were inhibitory at all but the lowest concentrations. Enzyme kinetics and docking simulations suggest that $[C_2C_1Im][OAc]$ and [Ch][Lys] may bind at the entrance to the active site to interfere with substrate interaction and catalysis, whereas $[DEA][HSO_4]$ likely does not. Both depolymerized and polymerized products were observed when the *TvL* enzyme was applied to a model GGE dimer and alkaline lignin in AILs. The reaction conditions still need to be optimized by using different lignins and thermophilic laccases with better resistance to AIL inhibition and higher temperatures. Collectively, this study provides a better understanding of the interactions between a fungal laccase and AILs and serves as a foundation for developing lignin valorization via biocatalysis in AILs.

ASSOCIATED CONTENT

Supporting Information

The Supporting Information is available free of charge on the ACS Publications website at DOI: 10.1021/acssuschemeng.9b02151.

Hanes−Woolf curves of *TvL* in ILs after linearization of Michaelis−Menten curves; proposed structure of model compound oligomers; chemical structure (FTIR) and thermal profiles (DSC) of alkaline lignin before and after treatment with laccase, ABTS, and ILs; molecular weight distribution of lignin streams before and after treatment with laccase, ABTS, and ILs; and full set of alkaline lignin HSQC before and after treatment with laccase, ABTS, and ILs (PDF)

AUTHOR INFORMATION

Corresponding Author

*E-mail: j.shi@uky.edu. Phone: (859) 218-4321. Fax: (859) 257-5671.

ORCID

Justin K. Mobley: 0000-0003-0394-6398

Bert C. Lynn: 0000-0001-8426-3024

Jian Shi: 0000-0003-3022-4446

Present Address

[‖]Biomass Science and Conversion Technology, Sandia National Laboratories, 7011 East Avenue, Livermore, CA, 94551, USA.

Notes

The authors declare no competing financial interest.

ACKNOWLEDGMENTS

The authors acknowledge the National Science Foundation under Cooperative Agreement nos. 1355438 and 1632854. This is a publication of the Kentucky Agricultural Experiment Station and is published with the approval of the Director. This work is also supported by the National Institute of Food and Agriculture, U.S. Department of Agriculture, Hatch-Multistate project under accession number 1003563.

REFERENCES

(1) Doherty, W. O. S.; Mousavioun, P.; Fellows, C. M. Value-adding to cellulosic ethanol: Lignin polymers. *Ind. Crops Prod.* **2011**, *33*, 259−276.

(2) Chatel, G.; Rogers, R. D. Review: Oxidation of Lignin Using Ionic Liquids—An Innovative Strategy To Produce Renewable Chemicals. *ACS Sustainable Chem. Eng.* **2014**, *2*, 322−339.

(3) Mamman, A. S.; Lee, J.-M.; Kim, Y.-C.; Hwang, I. T.; Park, N.-J.; Hwang, Y. K.; Chang, J.-S.; Hwang, J.-S. Furfural: Hemicellulose/xylosederived biochemical. *Biofuels, Bioprod. Biorefin.* **2008**, *2*, 438−454.

(4) Weng, J.-K.; Chapple, C. The origin and evolution of lignin biosynthesis. *New Phytol.* **2010**, *187*, 273−285.

(5) Vanholme, R.; Demedts, B.; Morreel, K.; Ralph, J.; Boerjan, W. Lignin Biosynthesis and Structure. *Plant Physiol.* **2010**, *153*, 895−905.

(6) Sette, M.; Wechselberger, R.; Crestini, C. Elucidation of Lignin Structure by Quantitative 2D NMR. *Chem.—Eur. J.* **2011**, *17*, 9529−9535.

(7) Zeng, J.; Helms, G. L.; Gao, X.; Chen, S. Quantification of Wheat Straw Lignin Structure by Comprehensive NMR Analysis. *J. Agric. Food Chem.* **2013**, *61*, 10848−10857.

(8) Suhas; Carrott, P. J. M.; Ribeiro Carrott, M. M. L. Lignin − from natural adsorbent to activated carbon: A review. *Bioresour. Technol.* **2007**, *98*, 2301−2312.

(9) Tilman, D.; Socolow, R.; Foley, J. A.; Hill, J.; Larson, E.; Lynd, L.; Pacala, S.; Reilly, J.; Searchinger, T.; Somerville, C.; Williams, R. Beneficial Biofuels—The Food, Energy, and Environment Trilemma. *Science* **2009**, *325*, 270−271.

(10) National Research Council; National Academy of Engineering; National Academy of Sciences. *Liquid Transportation Fuels from Coal and Biomass: Technological Status, Costs, and Environmental Impacts*; The National Academies Press: Washington, DC, 2009; p 388.

(11) Mottiar, Y.; Vanholme, R.; Boerjan, W.; Ralph, J.; Mansfield, S. D. Designer lignins: harnessing the plasticity of lignification. *Curr. Opin. Biotechnol.* **2016**, *37*, 190−200.

(12) Ragauskas, A. J.; Beckham, G. T.; Biddy, M. J.; Chandra, R.; Chen, F.; Davis, M. F.; Davison, B. H.; Dixon, R. A.; Gilna, P.; Keller, M.; Langan, P.; Naskar, A. K.; Saddler, J. N.; Tschaplinski, T. J.;

DOI: 10.1021/acssuschemeng.9b02151
ACS Sustainable Chem. Eng. 2019, 7, 15928−15938

Tuskan, G. A.; Wyman, C. E. Lignin Valorization: Improving Lignin Processing in the Biorefinery. *Science* **2014**, *344*, 1246843.
(13) Kleinert, M.; Barth, T. Towards a Lignincellulosic Biorefinery: Direct One-Step Conversion of Lignin to Hydrogen-Enriched Biofuel. *Energy Fuels* **2008**, *22*, 1371−1379.
(14) Cotoruelo, L. M.; Marqués, M. D.; Leiva, A.; Rodríguez-Mirasol, J.; Cordero, T. Adsorption of oxygen-containing aromatics used in petrochemical, pharmaceutical and food industries by means of lignin based active carbons. *Adsorption* **2011**, *17*, 539−550.
(15) Penkina, A.; Hakola, M.; Paaver, U.; Vuorinen, S.; Kirsimäe, K.; Kogermann, K.; Veski, P.; Yliruusi, J.; Repo, T.; Heinämäki, J. Solid-state properties of softwood lignin and cellulose isolated by a new acid precipitation method. *Int. J. Biol. Macromol.* **2012**, *51*, 939−945.
(16) Laskar, D. D.; Yang, B.; Wang, H.; Lee, J. Pathways for biomass-derived lignin to hydrocarbon fuels. *Biofuels, Bioprod. Biorefin.* **2013**, *7*, 602−626.
(17) Beckham, G. T.; Johnson, C. W.; Karp, E. M.; Salvachúa, D.; Vardon, D. R. Opportunities and challenges in biological lignin valorization. *Curr. Opin. Biotechnol.* **2016**, *42*, 40−53.
(18) Fujii, K.; Uemura, M.; Hayakawa, C.; Funakawa, S.; Kosaki, T. Environmental control of lignin peroxidase, manganese peroxidase, and laccase activities in forest floor layers in humid Asia. *Soil Biol. Biochem.* **2013**, *57*, 109−115.
(19) De Wild, P. J.; Huijgen, W. J. J.; Gosselink, R. J. A. Lignin pyrolysis for profitable lignocellulosic biorefineries. *Biofuels, Bioprod. Biorefin.* **2014**, *8*, 645−657.
(20) Linger, J. G.; Vardon, D. R.; Guarnieri, M. T.; Karp, E. M.; Hunsinger, G. B.; Franden, M. A.; Johnson, C. W.; Chupka, G.; Strathmann, T. J.; Pienkos, P. T.; Beckham, G. T. Lignin valorization through integrated biological funneling and chemical catalysis. *Proc. Natl. Acad. Sci. U.S.A.* **2014**, *111*, 12013−12018.
(21) Munk, L.; Sitarz, A. K.; Kalyani, D. C.; Mikkelsen, J. D.; Meyer, A. S. Can laccases catalyze bond cleavage in lignin? *Biotechnol. Adv.* **2015**, *33*, 13−24.
(22) Varman, A. M.; He, L.; Follenfant, R.; Wu, W.; Wemmer, S.; Wrobel, S. A.; Tang, Y. J.; Singh, S. Decoding how a soil bacterium extracts building blocks and metabolic energy from ligninolysis provides road map for lignin valorization. *Proc. Natl. Acad. Sci. U.S.A.* **2016**, *113*, E5802−E5811.
(23) Shi, J.; Sharma-Shivappa, R. R.; Chinn, M. S. Interactions between fungal growth, substrate utilization and enzyme production during shallow stationary cultivation of Phanerochaete chrysosporium on cotton stalks. *Enzyme Microb. Technol.* **2012**, *51*, 1−8.
(24) Brown, M. E.; Chang, M. C. Exploring bacterial lignin degradation. *Curr. Opin. Chem. Biol.* **2014**, *19*, 1−7.
(25) Bugg, T. D. H.; Ahmad, M.; Hardiman, E. M.; Rahmanpour, R. Pathways for degradation of lignin in bacteria and fungi. *Nat. Prod. Rep.* **2011**, *28*, 1883−1896.
(26) Klibanov, A. M. Improving enzymes by using them in organic solvents. *Nature* **2001**, *409*, 241−246.
(27) Mozhaev, V. V.; Khmelnitsky, Y. L.; Sergeeva, M. V.; Belova, A. B.; Klyachko, N. L.; Levashov, A. V.; Martinek, K. Catalytic activity and denaturation of enzymes in water/organic cosolvent mixtures. alpha-Chymotrypsin and laccase in mixed water/alcohol, water/glycol and water/formamide solvents. *Eur. J. Biochem.* **1989**, *184*, 597−602.
(28) Park, S.; Kazlauskas, R. J. Biocatalysis in ionic liquids−advantages beyond green technology. *Curr. Opin. Biotechnol.* **2003**, *14*, 432−437.
(29) Rogers, R. D.; Seddon, K. R. Ionic Liquids–Solvents of the Future? *Science* **2003**, *302*, 792−793.
(30) Patel, R.; Kumari, M.; Khan, A. B. Recent Advances in the Applications of Ionic Liquids in Protein Stability and Activity: A Review. *Appl. Biochem. Biotechnol.* **2014**, *172*, 3701−3720.
(31) Brennecke, J. F.; Maginn, E. J. Ionic liquids: Innovative fluids for chemical processing. *AIChE J.* **2001**, *47*, 2384−2389.
(32) Gutowski, K. E.; Broker, G. A.; Willauer, H. D.; Huddleston, J. G.; Swatloski, R. P.; Holbrey, J. D.; Rogers, R. D. Controlling the Aqueous Miscibility of Ionic Liquids: Aqueous Biphasic Systems of Water-Miscible Ionic Liquids and Water-Structuring Salts for Recycle, Metathesis, and Separations. *J. Am. Chem. Soc.* **2003**, *125*, 6632−6633.
(33) Verdía, P.; Brandt, A.; Hallett, J. P.; Ray, M. J.; Welton, T. Fractionation of lignocellulosic biomass with the ionic liquid 1-butylimidazolium hydrogen sulfate. *Green Chem.* **2014**, *16*, 1617−1627.
(34) Fort, D. A.; Remsing, R. C.; Swatloski, R. P.; Moyna, P.; Moyna, G.; Rogers, R. D. Can ionic liquids dissolve wood? Processing and analysis of lignocellulosic materials with 1-n-butyl-3-methylimidazolium chloride. *Green Chem.* **2007**, *9*, 63−69.
(35) Kilpeläinen, I.; Xie, H.; King, A.; Granstrom, M.; Heikkinen, S.; Argyropoulos, D. S. Dissolution of Wood in Ionic Liquids. *J. Agric. Food Chem.* **2007**, *55*, 9142−9148.
(36) George, A.; Brandt, A.; Tran, K.; Zahari, S. M. S. N. S.; Klein-Marcuschamer, D.; Sun, N.; Sathitsuksanoh, N.; Shi, J.; Stavila, V.; Parthasarathi, R.; Singh, S.; Holmes, B. M.; Welton, T.; Simmons, B. A.; Hallett, J. P. Design of low-cost ionic liquids for lignocellulosic biomass pretreatment. *Green Chem.* **2015**, *17*, 1728−1734.
(37) Liu, E.; Das, L.; Zhao, B.; Crocker, M.; Shi, J. Impact of Dilute Sulfuric Acid, Ammonium Hydroxide, and Ionic Liquid Pretreatments on the Fractionation and Characterization of Engineered Switchgrass. *BioEnergy Res.* **2017**, *10*, 1079.
(38) Das, L.; Xu, S.; Shi, J. Catalytic Oxidation and Depolymerization of Lignin in Aqueous Ionic Liquid. *Front. Energy* **2017**, *5*, 21.
(39) Yoshida, H. LXIII.-Chemistry of lacquer (Urushi). Part I. Communication from the Chemical Society of Tokio. *J. Chem. Soc., Trans.* **1883**, *43*, 472−486.
(40) An, H.; Xiao, T.; Fan, H.; Wei, D. Molecular characterization of a novel thermostable laccase PPLCC2 from the brown rot fungus Postia placenta MAD-698-R. *Electron. J. Biotechnol.* **2015**, *18*, 451−458.
(41) Kiiskinen, L.-L.; Kruus, K.; Bailey, M.; Ylösmäki, E.; Siika-aho, M.; Saloheimo, M. Expression of Melanocarpus albomyces laccase in Trichoderma reesei and characterization of the purified enzyme. *Microbiology* **2004**, *150*, 3065−3074.
(42) Hullo, M.-F.; Moszer, I.; Danchin, A.; Martin-Verstraete, I. CotA of Bacillus subtilis Is a Copper-Dependent Laccase. *J. Bacteriol.* **2001**, *183*, 5426−5430.
(43) Piontek, K.; Antorini, M.; Choinowski, T. Crystal Structure of a Laccase from the FungusTrametes versicolor at 1.90-Å Resolution Containing a Full Complement of Coppers. *J. Biol. Chem.* **2002**, *277*, 37663−37669.
(44) Semba, Y.; Ishida, M.; Yokobori, S.-i.; Yamagishi, A. Ancestral amino acid substitution improves the thermal stability of recombinant lignin-peroxidase from white-rot fungi, Phanerochaete chrysosporium strain UAMH 3641. *Protein Eng., Des. Sel.* **2015**, *28*, 221−230.
(45) Dong, S.; Mao, L.; Luo, S.; Zhou, L.; Feng, Y.; Gao, S. Comparison of lignin peroxidase and horseradish peroxidase for catalyzing the removal of nonylphenol from water. *Environ. Sci. Pollut. Res.* **2014**, *21*, 2358−2366.
(46) Glenn, J. K.; Morgan, M. A.; Mayfield, M. B.; Kuwahara, M.; Gold, M. H. An extracellular H2O2-requiring enzyme preparation involved in lignin biodegradation by the white rot basidiomycete Phanerochaete chrysosporium. *Biochem. Biophys. Res. Commun.* **1983**, *114*, 1077−1083.
(47) Arora, D. S.; Sharma, R. K. Ligninolytic fungal laccases and their biotechnological applications. *Appl. Biochem. Biotechnol.* **2010**, *160*, 1760−1788.
(48) d'Acunzo, F.; Galli, C.; Gentili, P.; Sergi, F. Mechanistic and steric issues in the oxidation of phenolic and non-phenolic compounds by laccase or laccase-mediator systems. The case of bifunctional substrates. *New J. Chem.* **2006**, *30*, 583−591.
(49) Gamelas, J. A. F.; Tavares, A. P. M.; Evtuguin, D. V.; Xavier, A. M. B. Oxygen bleaching of kraft pulp with polyoxometalates and laccase applying a novel multi-stage process. *J. Mol. Catal. B: Enzym.* **2005**, *33*, 57−64.
(50) Rico, A.; Rencoret, J.; del Río, J. C.; Martínez, A. T.; Gutiérrez, A. Pretreatment with laccase and a phenolic mediator degrades lignin

DOI: 10.1021/acssuschemeng.9b02151
ACS Sustainable Chem. Eng. 2019, 7, 15928−15938

and enhances saccharification of Eucalyptus feedstock. *Biotechnol. Biofuels* **2014**, *7*, 6.
(51) Moniruzzaman, M.; Kamiya, N.; Goto, M. Activation and stabilization of enzymes in ionic liquids. *Org. Biomol. Chem.* **2010**, *8*, 2887−2899.
(52) Du, J.; Shao, Z.; Zhao, H. Engineering microbial factories for synthesis of value-added products. *J. Ind. Microbiol. Biotechnol.* **2011**, *38*, 873.
(53) Attri, P.; Venkatesu, P.; Kumar, A. Activity and stability of [small alpha]-chymotrypsin in biocompatible ionic liquids: enzyme refolding by triethyl ammonium acetate. *Phys. Chem. Chem. Phys.* **2011**, *13*, 2788−2796.
(54) Naushad, M.; Alothman, Z. A.; Khan, A. B.; Ali, M. Effect of ionic liquid on activity, stability, and structure of enzymes: A review. *Int. J. Biol. Macromol.* **2012**, *51*, 555−560.
(55) Harwardt, N.; Stripling, N.; Roth, S.; Liu, H.; Schwaneberg, U.; Spiess, A. C. Effects of ionic liquids on the reaction kinetics of a laccase−mediator system. *RSC Adv.* **2014**, *4*, 17097.
(56) Galai, S.; de los Ríos, A. P.; Hernández-Fernández, F. J.; Haj Kacem, S.; Tomas-Alonso, F. Over-activity and stability of laccase using ionic liquids: screening and application in dye decolorization. *RSC Adv.* **2015**, *5*, 16173−16189.
(57) Re, R.; Pellegrini, N.; Proteggente, A.; Pannala, A.; Yang, M.; Rice-Evans, C. Antioxidant activity applying an improved ABTS radical cation decolorization assay. *Free Radicals Biol. Med.* **1999**, *26*, 1231−1237.
(58) Trott, O.; Olson, A. J. AutoDock Vina: Improving the speed and accuracy of docking with a new scoring function, efficient optimization, and multithreading. *J. Comput. Chem.* **2009**, *31*, 455−461.
(59) Das, A.; Rahimi, A.; Ulbrich, A.; Alherech, M.; Motagamwala, A. H.; Bhalla, A.; da Costa Sousa, L.; Balan, V.; Dumesic, J. A.; Hegg, E. L.; Dale, B. E.; Ralph, J.; Coon, J. J.; Stahl, S. S. Lignin conversion to low-molecular-weight aromatics via an aerobic oxidation-hydrolysis sequence: comparison of different lignin sources. *ACS Sustainable Chem. Eng.* **2018**, *6*, 3367−3374.
(60) Prado, R.; Brandt, A.; Erdocia, X.; Hallet, J.; Welton, T.; Labidi, J. Lignin oxidation and depolymerisation in ionic liquids. *Green Chem.* **2016**, *18*, 834−841.
(61) Guerra, A.; Lucia, L. A.; Argyropoulos, D. S. Isolation and characterization of lignins from Eucalyptus grandis Hill ex Maiden and Eucalyptus globulus Labill. by enzymatic mild acidolysis (EMAL). *Holzforschung* **2008**, *62*, 24.
(62) Rahimi, A.; Azarpira, A.; Kim, H.; Ralph, J.; Stahl, S. S. Chemoselective Metal-Free Aerobic Alcohol Oxidation in Lignin. *J. Am. Chem. Soc.* **2013**, *135*, 6415−6418.
(63) Liu, E.; Li, M.; Das, L.; Pu, Y.; Frazier, T.; Zhao, B.; Crocker, M.; Ragauskas, A. J.; Shi, J. Understanding Lignin Fractionation and Characterization from Engineered Switchgrass Treated by an Aqueous Ionic Liquid. *ACS Sustainable Chem. Eng.* **2018**, *6*, 6612−6623.
(64) Shi, J.; Balamurugan, K.; Parthasarathi, R.; Sathitsuksanoh, N.; Zhang, S.; Stavila, V.; Subramanian, V.; Simmons, B. A.; Singh, S. Understanding the role of water during ionic liquid pretreatment of lignocellulose: co-solvent or anti-solvent? *Green Chem.* **2014**, *16*, 3830−3840.
(65) Yuan, X.; Singh, S.; Simmons, B. A.; Cheng, G. Biomass Pretreatment Using Dilute Aqueous Ionic Liquid (IL) Solutions with Dynamically Varying IL Concentration and Its Impact on IL Recycling. *ACS Sustainable Chem. Eng.* **2017**, *5*, 4408−4413.
(66) Gschwend, F. J. V.; Malaret, F.; Shinde, S.; Brandt-Talbot, A.; Hallett, J. P. Rapid pretreatment of Miscanthus using the low-cost ionic liquid triethylammonium hydrogen sulfate at elevated temperatures. *Green Chem.* **2018**, *20*, 3486−3498.
(67) Dabirmanesh, B.; Khajeh, K.; Ghazi, F.; Ranjbar, B.; Etezad, S.-M. A semi-rational approach to obtain an ionic liquid tolerant bacterial laccase through π-type interactions. *Int. J. Biol. Macromol.* **2015**, *79*, 822−829.
(68) Shi, J.; Gladden, J. M.; Sathitsuksanoh, N.; Kambam, P.; Sandoval, L.; Mitra, D.; Zhang, S.; George, A.; Singer, S. W.; Simmons, B. A.; Singh, S. One-pot ionic liquid pretreatment and saccharification of switchgrass. *Green Chem.* **2013**, *15*, 2579−2589.
(69) Sun, J.; Konda, N. V. S. N. M.; Shi, J.; Parthasarathi, R.; Dutta, T.; Xu, F.; Scown, C. D.; Simmons, B. A.; Singh, S. CO 2 enabled process integration for the production of cellulosic ethanol using bionic liquids. *Energy Environ. Sci.* **2016**, *9*, 2822−2834.
(70) Xu, F.; Sun, J.; Wehrs, M.; Kim, K. H.; Rau, S. S.; Chan, A. M.; Simmons, B. A.; Mukhopadhyay, A.; Singh, S. Biocompatible Choline-Based Deep Eutectic Solvents Enable One-Pot Production of Cellulosic Ethanol. *ACS Sustainable Chem. Eng.* **2018**, *6*, 8914−8919.
(71) Fernández-Fernández, M.; Moldes, D.; Domínguez, A.; Sanromán, M. Á.; Tavares, A. P. M.; Rodríguez, O.; Macedo, E. A. Stability and kinetic behavior of immobilized laccase from Myceliophthora thermophila in the presence of the ionic liquid 1-ethyl-3-methylimidazolium ethylsulfate. *Biotechnol. Prog.* **2014**, *30*, 790.
(72) Rehmann, L.; Ivanova, E.; Ferguson, J. L.; Gunaratne, H. Q. N.; Seddon, K. R.; Stephens, G. M. Measuring the effect of ionic liquids on laccase activity using a simple, parallel method. *Green Chem.* **2012**, *14*, 725−733.
(73) Tavares, A. P. M.; Rodriguez, O.; Macedo, E. A. Ionic Liquids as Alternative Co-Solvents for Laccase: Study of Enzyme Activity and Stability. *Biotechnol. Bioeng.* **2008**, *101*, 201.
(74) Sun, J.; Liu, H.; Yang, W.; Chen, S.; Fu, S. Molecular Mechanisms Underlying Inhibitory Binding of Alkylimidazolium Ionic Liquids to Laccase. *Molecules* **2017**, *22*, 1353.
(75) Yang, Z. Hofmeister effects: an explanation for the impact of ionic liquids on biocatalysis. *J. Biotechnol.* **2009**, *144*, 12−22.
(76) Constantinescu, D.; Weingärtner, H.; Herrmann, C. Protein denaturation by ionic liquids and the Hofmeister series: a case study of aqueous solutions of ribonuclease A. *Angew. Chem., Int. Ed.* **2007**, *46*, 8887−8889.
(77) Zhao, H.; Olubajo, O.; Song, Z.; Sims, A. L.; Person, T. E.; Lawal, R. A.; Holley, L. A. Effect of kosmotropicity of ionic liquids on the enzyme stability in aqueous solutions. *Bioorg. Chem.* **2006**, *34*, 15−25.
(78) Jia, S.; Cox, B. J.; Guo, X.; Zhang, Z. C.; Ekerdt, J. G. Cleaving the β-O-4 Bonds of Lignin Model Compounds in an Acidic Ionic Liquid, 1-H-3-Methylimidazolium Chloride: An Optional Strategy for the Degradation of Lignin. *ChemSusChem* **2010**, *3*, 1078−1084.
(79) Lahtinen, M.; Kruus, K.; Heinonen, P.; Sipilä, J. On the reactions of two fungal laccases differing in their redox potential with lignin model compounds: products and their rate of formation. *J. Agric. Food Chem.* **2009**, *57*, 8357−8365.
(80) Rittstieg, K.; Suurnakki, A.; Suortti, T.; Kruus, K.; Guebitz, G. M.; Buchert, J. Polymerization of Guaiacol and a Phenolic β-O-4-Substructure by Trameteshirsuta Laccase in the Presence of ABTS. *Biotechnol. Prog.* **2003**, *19*, 1505−1509.
(81) Li, Q.; Xie, S.; Serem, W. K.; Naik, M. T.; Liu, L.; Yuan, J. S. Quality carbon fibers from fractionated lignin. *Green Chem.* **2017**, *19*, 1628−1634.
(82) Toledano, A.; Serrano, L.; Labidi, J. Improving base catalyzed lignin depolymerization by avoiding lignin repolymerization. *Fuel* **2014**, *116*, 617−624.
(83) Das, L.; Kolar, P.; Sharma-Shivappa, R. Heterogeneous catalytic oxidation of lignin into value-added chemicals. *Biofuels* **2012**, *3*, 155−166.
(84) Yao, S. G.; Mobley, J. K.; Ralph, J.; Crocker, M.; Parkin, S.; Selegue, J. P.; Meier, M. S. Mechanochemical treatment facilitates two-step oxidative depolymerization of kraft lignin. *ACS Sustainable Chem. Eng.* **2018**, *6*, 5990−5998.
(85) Crestini, C.; Lange, H.; Sette, M.; Argyropoulos, D. S. On the structure of softwood kraft lignin. *Green Chem.* **2017**, *19*, 4104−4121.

DOI: 10.1021/acssuschemeng.9b02151
ACS Sustainable Chem. Eng. 2019, 7, 15928−15938